Micromechanics of asperity rupture during laboratory stick slip experiments

Gregory C. McLaskey[1] and Steven D. Glaser[1]

Received 21 March 2011; revised 12 May 2011; accepted 14 May 2011; published 28 June 2011.

[1] Acoustic emissions and tremor-like signals are widely recorded in laboratory experiments. We are able to isolate the physical origins of these signals using high resolution nanoseismic analysis. The use of a picometer-sensitive, wide-band sensor array permits us to determine force-time functions and focal mechanisms for discrete events found amid the "noise" of friction, similar to how low frequency earthquakes are found buried within tremor. We interpret these localized events to be the rupture of μm-sized contacts, known as asperities. We performed stick-slip experiments on plastic/plastic and rock/rock interfaces and found a systematic difference between the nano earthquakes: the rock interface produces very rapid (<1 μs) implosive forces indicative of brittle failure and fault gouge formation, while rupture on the plastic interface releases only shear force and produces a nano quake more similar to earthquakes commonly recorded in the field. The difference between the mechanisms is attributed to the vast differences in the hardness and melting temperatures of the two materials, which affect the distribution of asperities as well as their failure behavior. With proper scaling, the strong link between material properties and laboratory earthquakes will aid in our understanding of fault mechanics and the generation of earthquakes and tectonic tremor. **Citation:** McLaskey, G. C., and S. D. Glaser (2011), Micromechanics of asperity rupture during laboratory stick slip experiments, *Geophys. Res. Lett.*, *38*, L12302, doi:10.1029/2011GL047507.

1. Introduction

[2] Modern studies of friction [*Brown et al.*, 1986; *Dieterich and Kilgore*, 1994; *Persson*, 1998; *Berthoud et al.*, 1999] have shown that "true" contact between two nominally flat surfaces consists of an ensemble of μm-scale contacts which collectively comprise only a small fraction of the apparent contact area. These, as well as seismological studies based on small repeating earthquakes [*Nadeau and McEvilly*, 1999; *Schaff and Beroza*, 2004], have motivated earthquake models [*Noda et al.*, 2009; *Johnson*, 2010] which paint a qualitatively similar picture of faults: nearly all fault strength is supplied by a sparse population of contacts known as asperities. Similarly, geometrical or frictional heterogeneities have been suggested as the source of tectonic tremor and low frequency earthquakes generated on an otherwise aseismically slipping fault [*Shelly et al.*, 2006].

[3] Due to their impulsive nature, acoustic emissions (AE) recorded in laboratory studies are usually considered to be somewhat analogous to earthquakes, and typical AE analysis tools are borrowed from seismology. The discovery of tectonic tremor [*Obara*, 2002], and evidence that it is generated by frictional slip [*Shelly et al.*, 2007; *Ide et al.*, 2007; *Wech and Creager*, 2007], has motivated recent lab experiments [*Zigone et al.*, 2011] which analyze continuous and less impulsive stress wave emission recorded during friction tests, in order to explore a possible analogue to tectonic tremor. In order to better interpret the results of these laboratory experiments, the precise physical origin of impulsive and continuous AE must be determined. In this study, we present the results of high resolution laboratory experiments which help constrain the physical origins of these signals.

2. Methods

[4] We study stick-slip behavior of two materials with vastly different physical properties: Poly(methyl methacrylate) (PMMA) and Academy Black granite (see Table 1). In contrast to previous studies, which rely on waveforms recorded with resonant sensors [*Sammonds and Ohnaka*, 1998; *Yabe et al.*, 2003; *Thompson et al.*, 2005; *Mair et al.*, 2007; *Yabe*, 2008; *Zigone et al.*, 2011] we employ an absolutely calibrated laboratory system instrumented with an array of wideband displacement sensors [*McLaskey and Glaser*, 2009]. These instruments detect surface normal displacements over the frequency band ~8 kHz – 2.5 MHz, with a ~1 picometer noise floor [*McLaskey and Glaser*, 2010]. This system allows us to study the full waveform of recorded signals, not just the timing and relative amplitude of tremor-like signals or the rise time and amplitude of initial P-wave arrivals. Our direct shear apparatus, schematically described in Figure 1a, consists of a slider block which is loaded onto a base plate with a constant and uniformly distributed normal force. An array of 13 sensors (S1–S13) located underneath the base plate detect high frequency seismic waves from a near-rupture vantage point.

[5] During a typical experiment, the shear force, F_S, is slowly increased until the block transitions from stick to slip. During each slip instability, an intense burst of waves are recorded with the nanoseismic sensor array. Details of one instability from a rock/rock test are shown in Figures 1b–1e. Analysis of these signals shows that the ~5–40 ms burst associated with the slip instability is composed of a multitude of discrete events on the order of 1 μs in duration (Figure 1d), many of which can be located and rigorously analyzed by their clearly identifiable P and S waves. For these tests on rock (Figure 1), recorded signals are described as tremor-like because they are extended in time and appear to lack coherent or impulsive wave arrivals. Upon close inspection, the signal is a cacophony of thousands of events recorded during each slip. By hand-picking unmistakable waveforms, we are

[1]Department of Civil and Environmental Engineering, University of California, Berkeley, California, USA.

0094-8276/11/2011GL047507

Table 1. Shear Modulus, Indentation Hardness, and Melting Temperature of the Two Materials Tested

	μ (GPa)	H_I (GPa)	T_m (°C)
Academy Black granite	27[a]	4–6[b]	750–1400[b]
PMMA	2.3[a]	0.3–0.5[c]	160[d]

[a]Estimated from measurements of shear wave velocity.
[b]*Spray* [2010].
[c]*Dieterich and Kilgore* [1994].
[d]*Smith and Hashemi* [2006].

usually able to study about fifty discrete events from amid the tremor-like signal; the rest were too small in amplitude relative to the noise of reflections from previous events to be evaluated with our methods. The location, timing, and amplitude of the events are shown in Figure 2. Additional experimental details are described in the auxiliary material.[1] In general, events were well distributed over a large portion of the nominal contact area with no space-time patterns, suggesting the sporadic rupture of discrete contacts.

[6] In contrast to the rock, which produced a tremor-like burst of exclusively high frequency (>100 kHz) signals, the stick-slip of the PMMA typically produced large amplitude lower frequency (<20 kHz) seismic waves with a few high frequency (>100 kHz) events riding on top of the lower frequency signal (details are shown in Figure S1 of the auxiliary material). Given the point source assumption inherent in our methodology, only the high frequency events were located and analyzed via the methods described in this paper.

3. Source Modeling

[7] When analyzing high frequency events from both PMMA and rock tests, the wide-band sensors detect sharp wave arrivals from both P and S waves, and this permits us to locate each event with ~mm spatial and ~μs temporal resolution. The focal mechanism and force-time history of the source are determined by matching full waveforms of the recorded signals to synthetic seismograms calculated with forward models that consider a wide range of source parameters. The suitability of the theoretical Green's functions [*Knopoff*, 1958; *Johnson*, 1974; *Hsu*, 1985] is verified by means of known calibration sources which are applied in situ, just before and after each experiment [*McLaskey and Glaser*, 2010] (see Figure S2 of the auxiliary material).

[8] We performed over fifty slip experiments on both the PMMA/PMMA and rock/rock interfaces, and varied the normal stress, shear loading rate, interfacial age, surface roughness, and sample geometry. For *all* of the high frequency (<100 kHz) events analyzed, focal mechanisms of PMMA/PMMA events are consistently different from those of rock/rock events. To illustrate this result, recorded signals shown in Figure 3 are compared to synthetic seismograms calculated for the best fit source models described in Figure 4. The events presented in Figures 3 and 4 are well constrained examples with good signal-to-noise ratio, but these mechanisms are representative of *all* of the high frequency (>100 kHz) events analyzed under the variety of conditions tested. We therefore attribute the differences in the focal mechanisms reported below to be material dependent rather than due to variation in experimental technique.

[9] Though the slider block and base plate appear to be in intimate contact, we find both the PMMA/PMMA and rock/rock interfaces to be acoustically highly reflective, and this affects the way in which the events must be modeled. Low frequency waves (<1 kHz) are transmitted across the fault, but stress waves in our detection range (~8 kHz – 2 MHz) are largely reflected. This is evidenced by multiple reflections through the thickness of the base plate, with lower frequency vibration modes clearly visible in Figure 3b. If the interface between the slider block and base plate were fully transparent, as is typically assumed in earthquake studies [*Aki and Richards*, 1980], the source should be modeled as a set of force couples, each with some time history f(t), acting within the interior of a body composed of both the base plate and slider block. Because the fault is reflective, it is effectively a free surface at high frequencies, and the wave field in the base plate is modeled as resulting from a single force f(t) acting on the interface, similar to the way landslides are modeled [*Kawakatsu*, 1989]. For a reflective fault, ground displacements from far field P and S waves are proportional to f(t), instead of df(t)/dt for a transparent fault.

[10] Synthetic seismograms (thin lines) are compared to recorded signals for both the PMMA/PMMA case (Figure 3a), and the rock/rock case (Figure 3b). White arrows in Figure 4 inset, show the direction of the force; f(t) is modeled as a step function of amplitude 90 mN and rise time 500 ns for the rock event and 50 mN/3 μs for PMMA event. For both the PMMA and rock, recorded P- and S-wave arrivals are step shaped (though the 20 kHz high-pass filtering causes them to appear somewhat like pulses in Figure 3), therefore f(t) is a step. This time history means that the events are due to a sudden release of force (~1–100 mN). PMMA events correspond to the release of shear force only. Rock events are due to the release of both shear and normal forces carried by the asperities.

4. Results and Discussion

[11] For the rock, the radiation pattern indicates a unidirectional implosion, with the direction of implosion oriented at an angle of ϕ = 0–60° from the fault normal (Figure 4b inset), and is inconsistent with both sliding and tensile crack opening mechanisms. All rock events had rise times of less than 1 μs. This very sudden release of normal force suggests that asperities do not simply slide past each other but fail in a brittle and catastrophic manner such as grain cataclasis during the formation of fault gouge. This conclusion is also supported by the observation of finely comminuted wear particles (gouge) found on the rock/rock interface after the stick-slip experiments. While consistent with some studies of mining-induced tremor, which found a significant implosive component to the source [*McGarr*, 1992], the focal mechanism results for the rock samples differ from earlier laboratory friction studies [*Yabe et al.*, 2003; *Thompson et al.*, 2005] that have suggested double-couple type sources. This difference might be due to the low normal stress of the current experiments (~100 kPa) relative to previous studies (typically ~10 MPa), which leads to a reduced density of asperities. Note that the quality of our recorded signals and the precise modeling of wave propagation effects allows the time history and focal mechanism of these sources to be

[1]Auxiliary materials are available in the HTML. doi:10.1029/2011GL047507.

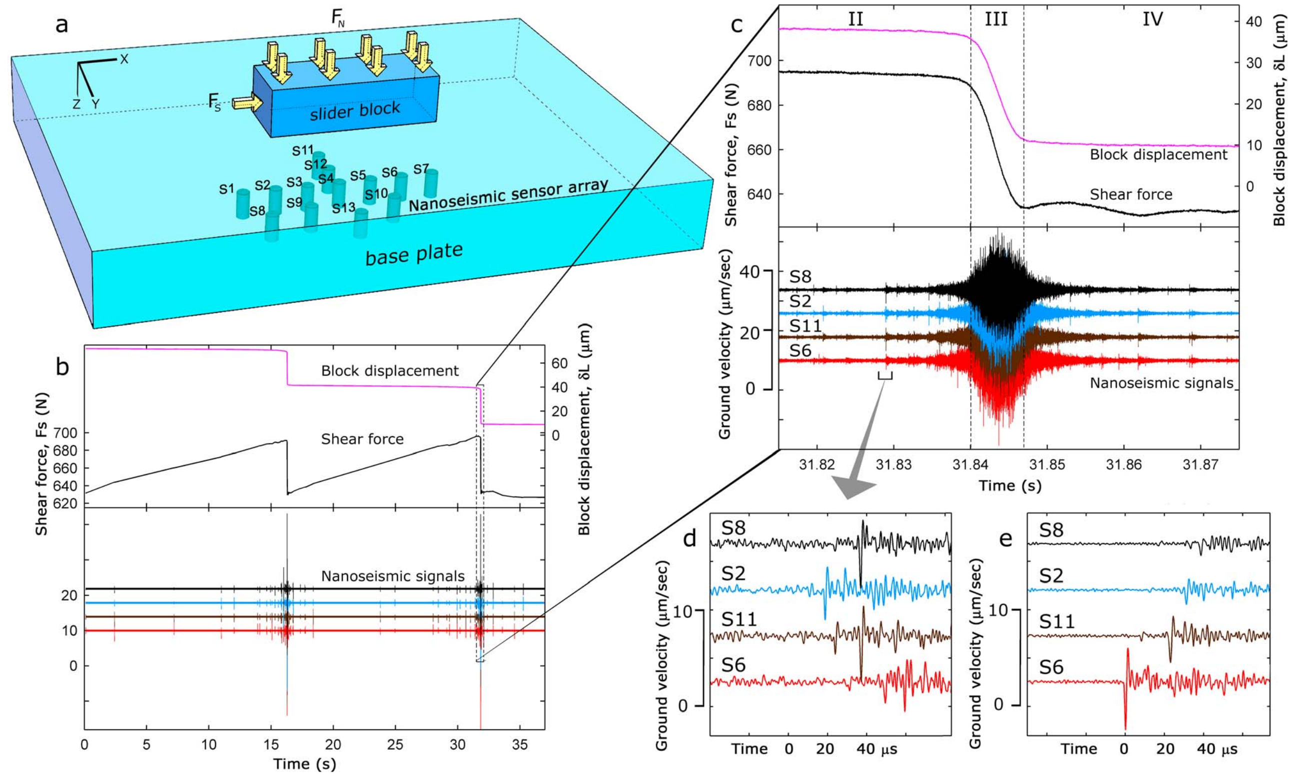

Figure 1. Schematic diagram of experimental configuration and typical results for a rock/rock interface. (a) A constant normal force, F_N, loads the slider block onto the base plate. An array of 13 sensors is located directly underneath the base plate. Shear force, F_S, applied to the trailing edge of the slider block, is slowly increased until the block slides in repeated stick-slip fashion. (b) Shear force and slider block displacement relative to the base plate, δ_L, are shown for two full stick-slip cycles along with simultaneous measurements of the radiated elastic waves, denoted 'nanoseismic signals'. (c) Details of one stick-slip instability show that the recorded signals consist of a multitude of discrete events. (d, e) Single events shown in more detail illustrating rapid (~μs) P- and S-wave arrivals. In Figures 1b–1e, recorded displacement signals have been differentiated to produce velocity. The event shown in Figure 1e is from an 'aftershock' occurring 0.2 seconds after the macroscopic slip instability shown in Figure 1c.

constrained with previously unachievable detail. The implosive sources described here may be due the fracture of individual asperities while the mechanisms described in previous studies are due to the coherent failure of many neighboring asperities.

[12] Asperity rupture on the PMMA/PMMA interface releases only shear force and produces a radiation pattern which is consistent with the double couple source commonly found in seismic studies. It is at first surprising to find that the PMMA events are more reminiscent of natural

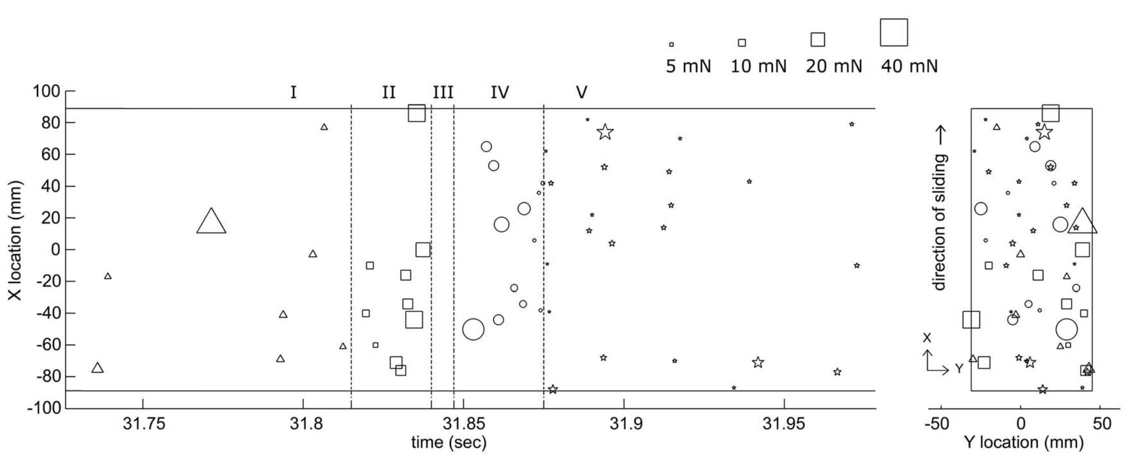

Figure 2. The locations, timing, and amplitude of 53 events located in a 300 ms time window surrounding the rock/rock slip instability shown in Figure 1. The timing of events is coded by symbol and the size of the symbol indicates the amplitude. Time periods II, III, and IV correspond to those shown in Figure 1c.

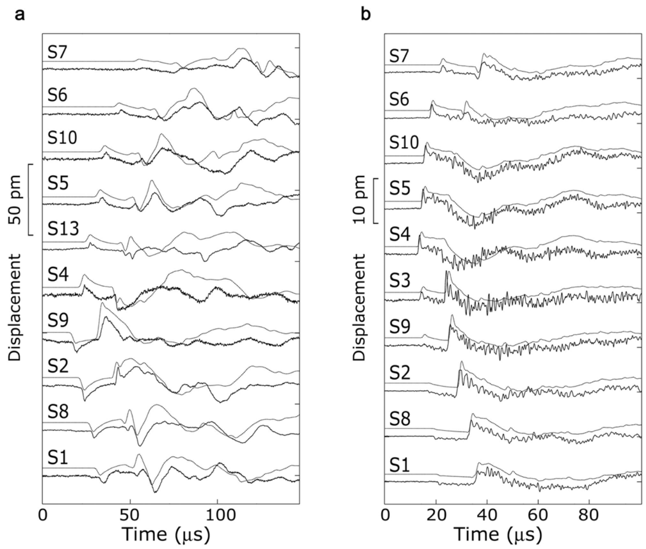

Figure 3. Comparison between recorded signals and synthetic seismograms (thin, dashed lines) calculated from models and sensor/source locations shown in Figure 4. (a) A typical event on PMMA/PMMA interface. (b) A typical event on rock/rock interface.

earthquakes than the rock. While the specimens of both materials were roughened in similar ways and subjected to similar stresses, the PMMA has a significantly lower indentation hardness than the rock (see Table 1), which affects asperity size and distribution. When normalized to the hardness of the material, even the low normal stress of the current experiments can produce an asperity population similar to that of many MPa in rock. Events studied from the PMMA/PMMA interface could be due to the coherent rupture of many micrometer-sized asperities, all located within our ~1 mm spatial resolution. The coherent rupture of asperity populations spanning larger areas could be the source of the lower frequency signals observed only for the PMMA.

[13] Besides differences in the hardness of the two materials, there are great differences in their melting temperatures. It has recently been suggested that PMMA asperities melt, or at least thermally weaken during shear [*Ben-David et al.*, 2010]. Flash heating of asperity contacts, suggested as a mechanism for dynamic fault weakening behavior [*Rice*, 2006; *Beeler et al.*, 2008], could be responsible for the similarity between the PMMA observed in this study and fault behavior commonly observed in the field. Additionally, we observed that for the PMMA, all high frequency events, and the majority of all seismic energy recorded, is coincident with the initiation of sliding. This suggests that high frequency seismic radiation is primarily produced during the initial rupture of asperities, and that a fault continues to slide, perhaps with melt as a lubricant, without releasing additional high frequency seismic energy. In contrast, the rock continued to produce high frequency events throughout slip. While it is rarely feasible to perform laboratory tests at confining pressures, loading rates, and temperatures common to natural, seismogenic, faults, this study suggests that informed material selection may be an effective substitute, to reproduce certain aspects of earthquake behavior.

[14] The quality of the waveforms recorded with our apparatus allows us to confidently image the complex dynamics of frictional sliding, so links can be made between measurable material behavior and the generation of (nano) earthquakes. We conclude that the rock interface slides as a sustained burst of implosive events with shear components which produce a remarkably tremor-like signal, while the much softer PMMA interface rapidly releases shear force upon rupture and produces seismic signatures more consistent with earthquakes, but then continues to slide aseismically. The signals described as tremor-like in this paper may be somewhat representative of tectonic tremor because they are composed of the superposition of many small events,

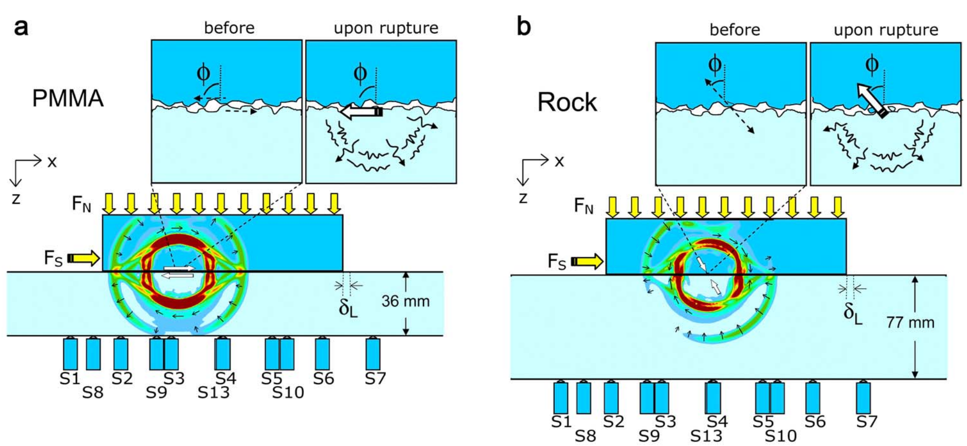

Figure 4. Schematic diagrams of source radiation patterns and associated micromechanical models of asperity failure. Dashed arrows represent the effectively static resisting forces which prevent the block from sliding. When the asperity ruptures, a very rapid reorganization of stress occurs. The white arrow represents the force felt by the base plate when the asperity ruptures which results in the high frequency stress wave radiation pattern shown in Figure 3. (a) On the PMMA, asperity rupture causes a rapid release of shear force, but the total normal force carried by the asperity is not rapidly changed. (b) For rock, asperity rupture relieves both shear and normal force in a unidirectional implosion indicative of brittle failure of the asperity.

which, on the whole, appear to lack coherent wave arrivals. But tectonic tremor is composed of low frequency earthquakes (LFEs), with notably different seismic spectra from regular earthquakes [*Shelly et al.*, 2006, 2007], and the physical origins of the differences between LFEs and typical earthquakes remain unresolved. The current comparison between rock and plastic suggests that tremor-like signals are produced by the sporadic and incoherent failure of widely-spaced asperities, while more impulsive, earthquake-like signals are produced by a more coherent rupture of closely spaced asperities.

[15] **Acknowledgments.** We thank L. Johnson and R. Burgmann for discussions and reading of the manuscript. This work was funded by NSF grant CMS-0624985.

[16] The Editor thanks Andre Niemeijer and an anonymous reviewer for their assistance in evaluating this paper.

References

Aki, K., and P. Richards (1980), *Quantitative Seismology: Theory and Methods*, Freeman, San Francisco, Calif.

Beeler, N., T. Tullis, and D. Goldsby (2008), Constitutive relationships and physical basis of fault strength due to flash heating, *J. Geophys. Res.*, *113*, B01401, doi:10.1029/2007JB004988.

Ben-David, O., S. Rubinstein, and J. Fineberg (2010), Slip-stick and the evolution of frictional strength, *Nature*, *463*, 76–79, doi:10.1038/nature08676.

Berthoud, P., T. Baumberger, C. G'Sell, and J.-M. Hiver (1999), Physical analysis of the state- and rate-dependent friction law: Static friction, *Phys. Rev. B*, *59*, 14,313–14,327, doi:10.1103/PhysRevB.59.14313.

Brown, S., R. Kranz, and B. Bonner (1986), Correlation between the surfaces of natural rock joints, *Geophys. Res. Lett.*, *13*, 1430–1433, doi:10.1029/GL013i013p01430.

Dieterich, J., and B. Kilgore (1994), Direct observations of frictional contacts—New insights for state-dependent properties, *Pure Appl. Geophys.*, *143*, 283–302, doi:10.1007/BF00874332.

Hsu, N. (1985), Dynamic Green's functions of an infinite plate—A computer program, *Tech. Rep. NBSIR 85–3234*, Cent. for Manuf. Eng., Natl. Bur. of Stand., Gaithersburg, Md.

Ide, S., D. Shelly, and G. Beroza (2007), Mechanism of deep low frequency earthquakes: Further evidence that deep non-volcanic tremor is generated by shear slip on the plate interface, *Geophys. Res. Lett.*, *34*, L03308, doi:10.1029/2006GL028890.

Johnson, L. (1974), Green's function for Lamb's problem, *Geophys. J. R. Astron. Soc.*, *37*, 99–131.

Johnson, L. (2010), An earthquake model with interacting asperities, *Geophys. J. Int.*, *182*, 1339–1373, doi:10.1111/j.1365-246X.2010.04680.x.

Kawakatsu, H. (1989), Centroid single force inversion of seismic waves generated by landslides, *J. Geophys. Res.*, *94*, 12,363–12,374, doi:10.1029/JB094iB09p12363.

Knopoff, L. (1958), Surface motions of a thick plate, *J. Appl. Phys.*, *29*, 661–670, doi:10.1063/1.1723246.

Mair, K., C. Marone, and P. Young (2007), Rate dependence of acoustic emissions generated during shear of simulated fault gouge, *Bull. Seismol. Soc. Am.*, *97*, 1841–1849, doi:10.1785/0120060242.

McGarr, A. (1992), An implosive component in the seismic moment tensor of a mining induced tremor, *Geophys. Res. Lett.*, *19*, 1579–1582, doi:10.1029/92GL01581.

McLaskey, G., and S. Glaser (2009), Nanoseismic measurement of the localized initiation of sliding friction, in *Meso-scale Shear Physics in Earthquake and Landslide Mechanics*, edited by Y. Hatzor et al., pp. 31–42, CRC Press, Boca Raton, Fla., doi:10.1201/b10826-6.

McLaskey, G., and S. Glaser (2010), Hertzian impact: Experimental study of the force pulse and resulting stress waves, *J. Acoust. Soc. Am.*, *128*, 1087–1096, doi:10.1121/1.3466847.

Nadeau, R., and T. McEvilly (1999), Fault slip rates at depth from recurrence intervals of repeating microearthquakes, *Science*, *285*, 718–721, doi:10.1126/science.285.5428.718.

Noda, H., E. Dunham, and J. Rice (2009), Earthquake ruptures with thermal weakening and the operation of major faults at low overall stress levels, *J. Geophys. Res.*, *114*, B07302, doi:10.1029/2008JB006143.

Obara, K. (2002), Nonvolcanic deep tremor associated with subduction in southwest Japan, *Science*, *296*, 1679–1681, doi:10.1126/science.1070378.

Persson, B. (1998), *Sliding Friction*, Springer, Berlin.

Rice, J. (2006), Heating and weakening of faults during earthquake slip, *J. Geophys. Res.*, *111*, B05311, doi:10.1029/2005JB004006.

Sammonds, P., and M. Ohnaka (1998), Evolution of microseismicity during frictional sliding, *Geophys. Res. Lett.*, *25*, 699–702, doi:10.1029/98GL00226.

Schaff, D., and G. Beroza (2004), Coseismic and postseismic velocity changes measured by repeating earthquakes, *J. Geophys. Res.*, *109*, B10302, doi:10.1029/2004JB003011.

Shelly, D., G. Beroza, S. Ide, and S. Nakamula (2006), Low-frequency earthquakes in Shikoku, Japan, and their relationship to episodic tremor and slip, *Nature*, *442*, 188–191, doi:10.1038/nature04931.

Shelly, D., G. Beroza, and S. Ide (2007), Non-volcanic tremor and low-frequency earthquake swarms, *Nature*, *446*, 305–307, doi:10.1038/nature05666.

Smith, W., and J. Hashemi (2006), *Foundations of Materials Science and Engineering*, 4th ed., McGraw Hill, New York.

Spray, J. (2010), Frictional melting processes in planetary materials: From hypervelocity impact to earthquakes, *Annu. Rev. Earth Planet. Sci.*, *38*, 221–254, doi:10.1146/annurev.earth.031208.100045.

Thompson, B., P. Young, and D. Lockner (2005), Observations of premonitory acoustic emission and slip nucleation during stick slip experiment in smooth faulted Westerly granite, *Geophys. Res. Lett.*, *32*, L10304, doi:10.1029/2005GL022750.

Wech, A., and K. Creager (2007), Cascadia tremor polarization evidence for plate interface slip, *Geophys. Res. Lett.*, *34*, L22306, doi:10.1029/2007GL031167.

Yabe, Y. (2008), Evolution of source characteristics of AE events during frictional sliding, *Earth Planets Space*, *60*, e5–e8.

Yabe, Y., N. Kato, K. Yamamoto, and T. Hirasawa (2003), Effect of sliding rate on the activity of acoustic emission during stable sliding, *Pure Appl. Geophys.*, *160*, 1163–1189, doi:10.1007/s000240300000.

Zigone, D., C. Voisin, E. Larose, F. Renard, and M. Campillo (2011), Slip acceleration generates seismic tremor like signals in friction experiments, *Geophys. Res. Lett.*, *38*, L01315, doi:10.1029/2010GL045603.

S. D. Glaser and G. C. McLaskey, Department of Civil and Environmental Engineering, University of California, 621A Sutardja Dai Hall, Berkeley, CA 94720-1758, USA. (gcm8ster@gmail.com)